Elastic Wave Propagation in Monoclinic System Due to Transient Line Load

*Yong-Yun Kim

Abstract

In this paper, we study the response of several anisotropic systems to buried transient line loads. The problem is mathematically formulated based on the equations of motion in the constitutive relations. The load is in the form of a normal stress acting with arbitrary axis on the plane of monoclinic symmetry. Plane wave equation is coupled with vertical shear wave, longitudinal wave and horizontal shear wave. We first considered the equation of motion in reference coordinate system, where the line load is coincident with symmetry axis of the orthotropic material. Then the equation of motion is transformed with respect to general coordinate system with azimuthal angle by using transformation tensor. The load is first described as a body force in the equations of the motion for the infinite media and then it is mathematically characterized. Subsequently the results for semi-infinite spaces is also obtained by using superposition of the infinite medium solution together with a scattered solution from the free surface. Consequently explicit solutions for the displacements are obtained by using Cargniard-DeHoop contour. Numerical results which are drawn from concrete examples of orthotropic material belonging to monoclinic symmetry are demonstrated.

I. Introduction

Elastic wave interaction with homogeneous elastic anisotropic media, in general, and with layered anisotropic media, in particular, have been extensively investigated in the past decade or so. This advancement has been prompted at least from a mechanics point of view, by the increased use of advanced composite materials in many structural applications. The effect of imposed line load in homogeneous isotropic media has been discussed by several investigators ever since Lord Rayleigh discovered the existence of surface waves on the surfaces of solids [1]. An account of the literature dealing with this problem through 1957 can be found in Ewing, Jardetzky and Press [2]. Most of the earlier work [2-4] followed Lamb [5], who apparently was the first to consider the motion of half space caused by a vertically applied line load on the free surface or within the isotropic medium. He was able to show that displacements at large distance consist of a series of events which corresponds to the arrival of longitudinal, shear, and Rayleigh surface waves. For a transient source loading results can be obtained from those corresponding to harmonic ones by a Fourier integral approach. The resulting double integral could be evaluated only by considering large distance. However, a suitable deformation of the integral contour by Cargniard-DeHoop not only resulted in considerable analytical simplification but led to exact, closed algebraic expression for the displacement of time [6].

In this paper, the formal developments in previous works are rigorously followed [7-10] and we study the response of monoclinic system to buried transient line loads. The load is first described as a body force in the equations of the motion for the infinite media and then it is mathematically characterized as "artificial interface conditions" for each semi-infinite spaces. A building block approach is utilized in which the analysis has begun by deriving the results for an infinite media. Subsequently the results for semi-infinite spaces, by using superposition of the infinite medium solution together with a scattered solution from the free surface. The sum of both solutions has to satisfy the stress free boundary conditions, thereby leading to a complete solution. Consequently explicit solutions for the displacements are obtained by using Cargniard-DeHoop contour. Numerical results which are drawn from concrete examples of orthotropic material, InAs, belonging to monoclinic symmetry are demonstrated.

II. Problem Formulation

Consider an infinite anisotropic elastic medium possessing orthotropic symmetry. The medium is oriented with respect to the reference cartesian coordinate system $x_i' = (x_1', x_2', x_3')$ such that the x_3' is assumed normal to its plane of symmetry as shown in Fig. 1. The plane of symmetry defining the orthotropic symmetry is thus coincident with the $x_1' - x_2'$ plane. With respect to this coordinate system, the equations of motion in the medium are given by

* Samsung Aerospace Industries Ltd., Precision Instruments R & D Center

Manuscript Received : August 5, 1998.

$$\frac{\partial \sigma_{ij}'}{\partial x_j'} + f_i' = \rho' \frac{\partial^2 u_i'}{\partial t^2} \tag{2.1}$$

and, from the general constitutive relations for anisotropic media,

$$\sigma_{ij}' = c_{ijkl}' e_{kl}', \qquad i, j, k, l = 1, 2, 3 \tag{2.2}$$

by the specialized expanded matrix form to orthotropic media

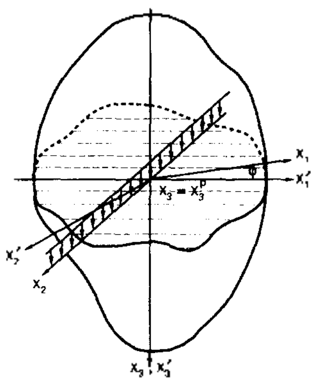

Figure 1. Line load in orthotropic infinite media.

$$\begin{Bmatrix} \sigma_{11}' \\ \sigma_{22}' \\ \sigma_{33}' \\ \sigma_{23}' \\ \sigma_{13}' \\ \sigma_{12}' \end{Bmatrix} = \begin{bmatrix} c_{11}' & c_{12}' & c_{13}' & 0 & 0 & 0 \\ c_{12}' & c_{22}' & c_{23}' & 0 & 0 & 0 \\ c_{13}' & c_{23}' & c_{33}' & 0 & 0 & 0 \\ 0 & 0 & 0 & c_{44}' & 0 & 0 \\ 0 & 0 & 0 & 0 & c_{55}' & 0 \\ 0 & 0 & 0 & 0 & 0 & c_{66}' \end{bmatrix} \begin{Bmatrix} e_{11}' \\ e_{22}' \\ e_{33}' \\ \gamma_{23}' \\ \gamma_{13}' \\ \gamma_{12}' \end{Bmatrix} \tag{2.3}$$

Where we used the standard contracted subscript notations $1 \to 11$, $2 \to 22$, $3 \to 33$, $4 \to 23$, $5 \to 13$ and $6 \to 12$, to replace fourth order tenser $c_{ijkl}\,(i, j, k, l = 1,2,3)$ with c_{pq} $(p, q = 1, 2, \ldots, 6)$. Thus, c_{45} stands for c_{2313}, for example. Here σ_{ij}, e_{ij} and u_i are the components of stress, strain and displacement, respectively, and ρ is the material density. In equation (2.3), $\gamma_{ij} = 2e_{ij}(i \neq j)$ defines the engineering shear strain components.

In what follows, we study of the infinite medium to a transient line load that is applied along a direction that makes an arbitrary azimuthal angle ϕ with the x_1' axis. Since the response of the medium to such a wave is independent of the applied line direction, we conduct our analysis in a transformed coordinate system x_i formed by a rotation of the plane $x_1' - x_2'$ through the angle ϕ about the x_3' axis. Thus, the direction x_2 will coincide with the line load direction. Since c_{ijkl} is a fourth order tensor, then for any orthogonal transformation of the primed to the non-primed coordinates, i.e., it transforms according to

$$c_{ijkl} = \beta_{im}\beta_{jn}\beta_{ko}\beta_{lp}c_{mnop}' \tag{2.4}$$

where β_{ij} is the cosine of the angle between x_i and x_i', respectively. For a rotation of angle ϕ in the $x_1' - x_2'$ plane, the transformation tensor β_{ij} reduces to

$$\beta_{ij} = \begin{vmatrix} \cos\phi & \sin\phi & 0 \\ -\sin\phi & \cos\phi & 0 \\ 0 & 0 & 1 \end{vmatrix} \tag{2.5}$$

If the transformation is applied to Eq.(2.3), one gets

$$\begin{Bmatrix} \sigma_{11} \\ \sigma_{22} \\ \sigma_{33} \\ \sigma_{23} \\ \sigma_{13} \\ \sigma_{12} \end{Bmatrix} = \begin{bmatrix} c_{11} & c_{12} & c_{13} & 0 & 0 & c_{16} \\ c_{12} & c_{22} & c_{23} & 0 & 0 & c_{26} \\ c_{13} & c_{23} & c_{33} & 0 & 0 & c_{36} \\ 0 & 0 & 0 & c_{44} & c_{45} & 0 \\ 0 & 0 & 0 & c_{45} & c_{55} & 0 \\ c_{16} & c_{26} & c_{36} & 0 & 0 & c_{66} \end{bmatrix} \begin{Bmatrix} e_{11} \\ e_{22} \\ e_{33} \\ \gamma_{23} \\ \gamma_{13} \\ \gamma_{12} \end{Bmatrix} \tag{2.6}$$

The orthotropic system is transformed to monoclinic with nonzero constants of c_{16}, c_{26}, c_{36}, and c_{45}. And the secular equation (2.1) is written in the expanded form in terms of displacement components by applying the tensor transformation, Eq.(2.4)-Eq.(2.6)

$$\begin{aligned} &[c_{11}\frac{\partial^2}{\partial x_1^2} + c_{55}\frac{\partial^2}{\partial x_3^2}]u_1 + [c_{16}\frac{\partial^2}{\partial x_1^2} + c_{45}\frac{\partial^2}{\partial x_3^2}]u_2 \\ &\quad + \frac{\partial}{\partial x_3}(c_{13} + c_{55})\frac{\partial u_3}{\partial x_1} = \rho\frac{\partial^2 u_1}{\partial t^2} - f_1 \end{aligned} \tag{2.7a}$$

$$\begin{aligned} &[c_{16}\frac{\partial^2}{\partial x_1^2} + c_{45}\frac{\partial^2}{\partial x_3^2}]u_1 + [c_{66}\frac{\partial^2}{\partial x_1^2} + c_{44}\frac{\partial^2}{\partial x_3^2}]u_2 \\ &\quad + \frac{\partial}{\partial x_3}(c_{36} + c_{45})\frac{\partial u_3}{\partial x_1} = \rho\frac{\partial^2 u_2}{\partial t^2} - f_2 \end{aligned} \tag{2.7b}$$

$$\begin{aligned} &\frac{\partial}{\partial x_3}(c_{13} + c_{55})\frac{\partial u_1}{\partial x_1} + \frac{\partial}{\partial x_3}(c_{36} + c_{45})\frac{\partial u_2}{\partial x_1} \\ &\quad + [c_{55}\frac{\partial^2}{\partial x_1^2} + c_{33}\frac{\partial^2}{\partial x_3^2}]u_3 = \rho\frac{\partial^2 u_3}{\partial t^2} - f_3 \end{aligned} \tag{2.7c}$$

where f_i is defined as $f_1 = f_2 = 0$, $f_3 = Q\delta(x_1)\delta(x_3 - x_3^p)F(t)$ for the line load and Q is x_3 component.

III. Solutions by Fourier transform

Formal solutions are effectuated by applying the Fourier transform to these Eqs.(2.7a-c) in accordance with

$$\overline{u_i} = \int_0^{\infty} u_i e^{-pt} dt, \qquad \widehat{u_i} = \int_{-\infty}^{\infty} \overline{u_i} e^{-jp\eta x_1} dx_1 \qquad (3.1)$$

The general solution of the resulting differential equations is then sought in the form

$$\widehat{u_i} = U_i e^{-p\alpha x_3}, \qquad i = 1, 2, 3 \qquad (3.2)$$

The steps leading to formal solutions of Eqs.(2.7a-c) for each of the two semi-infinite spaces (See Fig.1) will be outlined [7]. Body force, f_i, first, deleted from Eqs.(2.7a-c), since the body force has been replaced by an "artificial interface condition", which is given by

$$\begin{aligned} c_{33}\frac{\partial u_3}{\partial x_3} &= -\frac{1}{2}Q\delta(x_1)F(t), \quad \text{for } x_3 \geq x_3^p \text{ at } x_3 = x_3^p \\ c_{33}\frac{\partial u_3}{\partial x_3} &= \frac{1}{2}Q\delta(x_1)F(t), \quad \text{for } x_3 \leq x_3^p \text{ at } x_3 = x_3^p \end{aligned} \qquad (3.3)$$

Infinite Media

The Eqs.(2.7a-c) lead to the characteristic equation in terms of U_i by substituting Eq.(3.1) and Eq.(3.2). The characteristic equation yields nontrivial solutions in U_i, thereby resulting in the sixth order algebraic equation in α, whose α's have the further properties,

$$\alpha_2 = -\alpha_1, \quad \alpha_4 = -\alpha_3, \quad \alpha_6 = -\alpha_5 \qquad (3.4)$$

Furthermore for each α, Eq.(3.3) yields the displacement amplitude ratio,

$$\begin{aligned} V_q &= V_{q+1} - U_{2q}/U_{1q} = -[\Lambda_{11}\Lambda_{23} - \Lambda_{12}\Lambda_{13}]/[\Lambda_{12}\Lambda_{23} - \Lambda_{22}\Lambda_{13}] \\ W_q &= -W_{q+1} = U_{3q}/U_{1q} = -[\Lambda_{12}\Lambda_{23} - \Lambda_{13}\Lambda_{22}]/[\Lambda_{23}\Lambda_{23} - \Lambda_{22}\Lambda_{33}] \end{aligned} \qquad (3.5)$$

where the Λ_{ij} is given in Appendix. Finally, using superposition, the formal solutions can be written for the displacements of Eqs.(2.7a-c) and their associated stress components using Eq.(3.2) as

$$\begin{aligned} (\widehat{u_1}, \widehat{u_2}, \widehat{u_3}) &= \sum_{q=1}^{6}(1, V_q, W_q)U_{1q}e^{-p\alpha_q(x_3 - x_3^p)} \\ (\widehat{\sigma_{33}}, \widehat{\sigma_{13}}, \widehat{\sigma_{23}}) &= \sum_{q=1}^{6} p(D_{1q}, D_{2q}, D_{3q})U_{1q}e^{-p\alpha_q(x_3 - x_3^p)} \end{aligned} \qquad (3.6)$$

where D_{iq} is given in Appendix.

The above solutions with their various properties can now be specialized to both artificial semi-infinite spaces by the following steps. Inspection of the above solutions indicate that each consists of three pairs of wave components, each pair propagating in mirror image fashion with respect to the interface, namely along positive and negative x_3 directions. Since propagation is expected to emanate from the interface into both media, one arbitrary reserves α_1, α_3 and α_5 for the lower half-space; the remaining one's, namely described with α_2, α_4 and α_6 for the upper one. A formal solution of the field equation in monoclinic media have been obtained with the unknown amplitudes U_{1q}. The amplitudes U_{1q} will be determined by implementing the artificial interface conditions Eq.(3.3). With these solutions for the wave amplitudes, solutions for infinite space can be written in terms of $q = 1, 3, 5$

$$\begin{aligned} (\widehat{u_1}, \widehat{u_2}, \widehat{u_3}) &= \sum_{q=1,3,5} (1, V_q, W_q)U_{1q}e^{-p\alpha_q|x_3 - x_3^p|} \\ (\widehat{\sigma_{33}}, \widehat{\sigma_{13}}, \widehat{\sigma_{23}}) &= \sum_{q=1,3,5} p(D_{1q}, D_{2q}, D_{3q})U_{1q}e^{-p\alpha_q|x_3 - x_3^p|} \\ &\text{for} \quad x_3 \geq x_3^p \end{aligned} \qquad (3.7a)$$

$$\begin{aligned} (\widehat{u_1}, \widehat{u_2}, \widehat{u_3}) &= \sum_{q=1,3,5} (-1, -V_q, W_q)U_{1q}e^{-p\alpha_q|x_3 - x_3^p|} \\ (\widehat{\sigma_{33}}, \widehat{\sigma_{13}}, \widehat{\sigma_{23}}) &= \sum_{q=1,3,5} p(-D_{1q}, D_{2q}, D_{3q})U_{1q}e^{-p\alpha_q|x_3 - x_3^p|} \\ &\text{for} \quad x_3 \leq x_3^p \end{aligned} \qquad (3.7b)$$

where the displacement amplitudes, U_{1q}, are given in Appendix

Semi-infinite Media

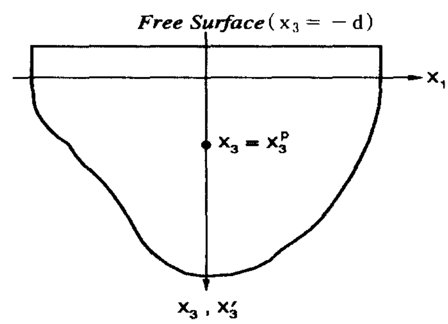

Figure 2. Semi-infinite media.

We now adapt the solutions of the infinite media Eq.(3.7a,b) to solve for the case where the free boundary intercepts the propagating pulse at some arbitrary location parallel to the plane $x_3 = 0$. It is assumed that the free boundary is located at $x_3 = -d$ as depicted in Fig. 2. This implies that the free boundary is located in the upper region and thus can only interfere with the propagation fields in the negative x_3 direction. For this case, the solution of Eq.(3.7a,b) will constitute an incident wave on a free surface. As a result, waves will reflect from the free boundary and propagate in the positive x_3 direction. Thus, appropriate formal solutions, superposing the incident waves and the reflected waves, can be adapted from the solution of Eq.(3.6) in accordance with

$$(\hat{u}_1^s, \hat{u}_2^s, \hat{u}_3^s) = (\hat{u}_1, \hat{u}_2, \hat{u}_3) + \sum_{q=1,3,5} (1, V_q, W_q) U_{1q}^r e^{p\alpha_q x_3}$$
$$(\hat{\sigma}_{33}^s, \hat{\sigma}_{23}^s, \hat{\sigma}_{13}^s) = (\hat{\sigma}_{33}, \hat{\sigma}_{23}, \hat{\sigma}_{13}) + \sum_{q=1,3} (D_{1q}, D_{2q}, D_{3q}) U_{1q}^r p e^{p\alpha_q(x_3 - x_1)} \tag{3.8}$$

The boundary condition on the free surface (Fig. 2) is given by

$$\hat{\sigma}_{13}^s = \hat{\sigma}_{23}^s = \hat{\sigma}_{33}^s = 0 \quad \text{at} \quad x_3 = -\mathrm{d} \tag{3.9}$$

By imposing the boundary condition on Eq.(3.8), we get the standard simultaneous linear equation. The reflected wave amplitudes are yielded, which are given in Appendix.

IV. Cargniard-DeHoop Contour variation

Now I will do the transformations back to the time-space domain by using Cargniard DeHoop method. The method is based on the following elementary property of the one-sided Laplace transform. First, consider the Laplace transform of u_i. $\overline{u}_i$ is obtained by

$$2\pi \overline{u}_i = \sum_{q=1,3,5} \int_{-\infty}^{\infty} U_{1q} e^{-p(\alpha_q x_3 - j\eta x_1)} d\eta \tag{4.1}$$

The integration in the complex η-plane is carried out along the paths where

$$t = \alpha x_3 - j\eta x_1 \quad \text{or} \quad \alpha = \frac{t + j\eta x_1}{x_3} \tag{4.2}$$

with t real and positive. Substitution of (3.2) into the characteristic equation yields the sixth order polynomial defining the Fourier parameter η ;

$$\Omega(x_1, x_3, t, \eta) = \sum_{n=0}^{6} B_n \eta^n = 0 \tag{4.3}$$

The six root is composed of three parabolas with respect to time t for a certain position (x_1, x_3), and they are symmetric about the imaginary η axis. Each of the parabolas is associated with four distinct roots of α from the characteristic equation, two of which correspond to the lower half-space and others to the upper half-space, because of the boundedness of the wave. Each of the two η represents a separate wavefront.

Infinite Media

Now the inverse Laplace transform can be obtained by mere inspection of Eq.(3.7a,b)

$$\frac{4\pi c_{55}}{Q} u_1 = [\frac{(V_5 - V_3)}{D_{um}}(\eta_1^+)\frac{\partial \eta_1^+}{\partial t} - \frac{(V_5 - V_3)}{D_{um}}(\eta_1^-)\frac{\partial \eta_1^-}{\partial t}] H(t - t_1) +$$
$$[\frac{(V_1 - V_5)}{D_{um}}(\eta_2^+)\frac{\partial \eta_2^+}{\partial t} - \frac{(V_1 - V_5)}{D_{um}}(\eta_2^-)\frac{\partial \eta_2^-}{\partial t}] H(t - t_2) +$$
$$[\frac{(V_3 - V_1)}{D_{um}}(\eta_3^+)\frac{\partial \eta_3^+}{\partial t} - \frac{(V_3 - V_1)}{D_{um}}(\eta_3^-)\frac{\partial \eta_3^-}{\partial t}] H(t - t_3) \tag{4.4}$$

The t_1, t_2 and t_3 are the arrival times of the wave fronts. In other words, they are the times that correspond to the values of the imaginary η axis intercepts of the two branches of η. The notation η^+ denotes the branch of η_i to the right side of the imaginary η axis and η^- denotes the branch of η_i to the left side of the imaginary η axis. By using same technique the displacement of u_2 and u_3 are obtained similarly to u_1, with multiplication of amplitude ratio, V_q, W_q, respectively, i.e $(V_5 - V_3)V_1/D_{um}$ for u_2, and $(V_5 - V_3)W_1/D_{um}$ for u_3.

Semi-Infinite Media

By the same procedure, integral transform solutions of Eq.(3.8) in the semi-infinite media are inversely transformed back to the space-time domain. The result of the wave propagation is given by

$$\frac{4\pi c_{55}}{Q} u_1^s = [\frac{(V_5 - V_3)(D_{sm} + (D_{11}G_1^u - D_{21}G_3^u - D_{31}G_5^u)D_{um})}{D_{um}D_{sm}}(\eta_1^+)\frac{\partial \eta_1^+}{\partial t} -$$
$$\frac{(V_5 - V_3)(D_{sm} + (D_{11}G_1^u - D_{21}G_3^u - D_{31}G_5^u)D_{um})}{D_{um}D_{sm}}$$
$$(\eta_1^-)\frac{\partial \eta_1^-}{\partial t}] H(t - t_1)$$
$$+ [\frac{(V_1 - V_5)(D_{sm} + (D_{13}G_1^u - D_{23}G_3^u - D_{33}G_5^u)D_{um})}{D_{um}D_{sm}}(\eta_2^+)\frac{\partial \eta_2^+}{\partial t}$$
$$\frac{(V_1 - V_5)(D_{sm} + (D_{13}G_1^u - D_{23}G_3^u - D_{33}G_5^u)D_{um})}{D_{um}D_{sm}}$$
$$(\eta_2^-)\frac{\partial \eta_2^-}{\partial t}] H(t - t_2)$$
$$+ [\frac{(V_3 - V_1)(D_{sm} + (D_{15}G_1^u - D_{25}G_3^u - D_{35}G_5^u)D_{um})}{D_{um}D_{sm}}(\eta_3^+)\frac{\partial \eta_3^+}{\partial t} -$$
$$\frac{(V_3 - V_1)(D_{sm} + (D_{15}G_1^u - D_{25}G_3^u - D_{35}G_5^u)D_{um})}{D_{um}D_{sm}}$$
$$(\eta_3^-)\frac{\partial \eta_3^-}{\partial t}] H(t - t_3) \tag{4.5}$$

where $G_r^u = \sum_{q=1,3,5} G_{qr}$, $G_r^v = \sum_{q=1,3,5} G_{qr} V_q$,

$$G_r^w = \sum_{q=1,3,5} G_{qr} W_q, \quad r = 1,3,5$$

G_{qr} is given in Appendix. The remaining displacements u_2^s and u_3^s will be obtained by the same procedures.

VI. Numerical illustration and Discussion

Numerical illustrations are presented for the analysis. An InAs cubic material is chosen and its material constants are given by $c_{11}' = c_{22}' = c_{33}' = 83.29\times10^{10}$ N/m^2, $c_{12}' = c_{13}' = c_{23}' = 45.26\times10^{10}$ N/m^2, $c_{44}' = c_{55}' = c_{66}' = 39.59\times10^{10}$ N/m^2 and $\rho = 5.67$ g/cm^3. For a rotation of $\phi = 30°$, these properties transform to $c_{11} = c_{22} = 51.2\times10^{10}$ N/m^2, $c_{33} = 16.0\times10^{10}$ N/m^2, $c_{12} = 36.3\times10^{10}$ N/m^2, $c_{13} = c_{23} = 4.0\times10^{10}$ N/m^2, $c_{36} = 0.3\times10^{10}$ N/m^2, $c_{16} = c_{26} = 36.1\times10^{10}$ N/m^2, $c_{44} = c_{55} = 6.6\times10^{10}$ N/m^2, $c_{66} = 40.0\times10^{10}$ N/m^2. It confirms the earlier conclusion that the transformed matrix takes the format of monoclinic symmetry. Fig. 3 presents snap shot of absolute value of radical displacement field for infinite space corresponding to chosen azimuthal angle $\phi = 30°$ on $x_1 - x_3$ plane at fixed time ($t = 0.2\mu$sec). A spatial grid of 100×100 points is generated for the first quadrant. The remaining quadrants are then generated by the mirror of the first quadrant. The vertical line load is located at the origin that is the center of the picture. Since the medium is homogeneous, the wave field does not change as it propagates. The color scheme runs from white (minimum) to black (maximum). In this picture we can clearly recognize the wave curves (three wave fronts and lacunae). The picture shows that the contribution of the longitudinal wave is strong at $\theta = 0°$ whereas that of the shear wave is strong at $\theta = 90°$.

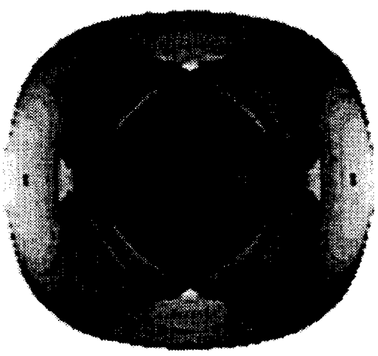

Figure 3. Snap shot of displacement field at $t = 0.2\mu$sec of InAs infinite system of $\phi = 30°$.

Fig. 4 presents snap shot of absolute value of radical displacement fields on $x_1 - x_3$ plane of semi-infinite space corresponding to $\phi = 30°$ at fixed time (t=0.2μsec). In this figure, we can clearly recognize the wave curves (surface wave and three bulk wave forms). The surface wave peaks are shown at inside of the longitudinal wave front and near the horizontal plane surface.

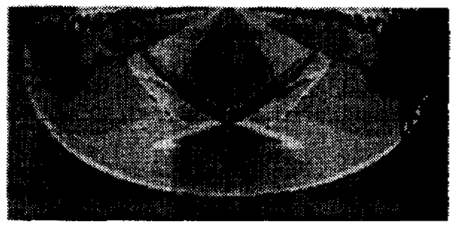

Figure 4. Snap shot of displacement field at $t = 0.2\mu$sec of semi- infinite system

VII. Conclusion

Explicit solutions for the displacements due to transient line loads, which include infinite, semi-infinite spaces for the monoclinic system, are obtained by using Cargniard-DeHoop contour. Numerical results which are drawn from concrete examples of orthotropic symmetry are demonstrated. Wave equation is coupled with vertical shear wave, longitudinal wave and horizontal shear wave. As the azimuthal angle approaches to zero, horizontal shear wave components disappear and other wave components have numerical results close to those in orthotropic system. But wave components can't be numerically calculated by using final solutions in monoclinic system since the displacement ratio V_q have always zero value in case of the orthotropic system which banish all the displacement amplitudes. So analytical solutions for orthotropic system have to be driven by decoupling horizontal shear wave, which will be adquate for the material system possessing orthotropic or higher symmetry, transversely isotropic, cubic, and isotropic symmetry. The solutions of the system with orthotropic symmetry will be simplified to those of isotropic systems by exploiting elastic properties of λ and μ, also.

References

1. Lord Rayleigh, "On the free vibrations of an infinite plate of homogeneous isotropic elastic material," Proc. London Mathematical society, 20, pp.225, 1889.
2. W. Ewing, W. Jardetzky and F. Press, Elastic media, McGraw Hill, New York, 1957.
3. G. Eason, J. Fulton and I. N. Sneddon, "The generation of wave in an infinite elastic solid by variable body forces," *Phil. Trans. Roy. Soc., London, Ser. A*, Vol.248, pp. 575-308, 1956.

4. E. R. Lapwood, "The disturbance due to a line source in a semi-infinite elastic medium," Phil. Trans. Roy. Soc., London, Ser. A, Vol. 242, pp.9-100, 1949.
5. H. Lamb, "On waves in an elastic plate," *Phil. Trans. Roy Soc., London, Ser. A*, Vol. 93, pp124-128, 1917.
6. A. T. De Hoop, "A modification of Cargniard's Method for solving Seismic pulse problems," *Appli.sci.Res., B*, Vol. 8 pp.349-357, 1960.
7. Y. Y. Kim, "Elastic waves in anisotropic media," Ph.D. Dissertation, University of Cincinnati, 1993.
8. D. E. Chimenti and A. H. Nayfeh, "Ultrasonic reflection and guided waves in fluid-coupled composite laminates," *J. Nondestructive evaluation*, Vol. 9, No. 2/3, 1990.
9. A. H. Nayfeh and D. E. Chimenti, "Propagation of guided waves in fluid-coupled composite plates of fiber-reinforced composites," *J. Appl. Mech.*, Vol. 83, pp1736, 1988.
10. D. E. Chimenti and A. H. Nayfeh, "Ultrasonic leaky waves in a solid plate separating fluid and vacuum media," *J. Acous. Soc. Am.*, Vol. 85, pp2, 1989.

Appendix

Various coefficients are given by

$$A_{11} = c_{55}\alpha^2 - c_{11}\xi^2 + \rho\omega^2$$
$$A_{12} = c_{45}\alpha^2 - c_{16}\xi^2$$
$$A_{13} = -j\xi\alpha(c_{13} + c_{55})$$
$$A_{22} = c_{44}\alpha^2 - c_{66}\xi^2 + \rho\omega^2$$
$$A_{23} = -j\xi\alpha(c_{36} + c_{45})$$
$$A_{33} = c_{33}\alpha^2 - c_{55}\xi^2 + \rho\omega^2$$

$$D_{1q} = j\xi(c_{13} + c_{36}V_q) - c_{33}\alpha_q W_q$$
$$D_{2q} = c_{55}(j\xi W_q - \alpha_q) - c_{45}\alpha_q V_q$$
$$D_{3q} = c_{45}(j\xi W_q - \alpha_q) - c_{44}\alpha_q V_q, \quad q = 1, 2, 3, 4, 5, 6$$

$$U_{11} = -U_{12} = \overline{F(p)}(V_5 - V_3)Q/(2c_{33}D_{um}p)$$
$$U_{13} = -U_{14} = \overline{F(p)}(V_1 - V_5)Q/(2c_{33}D_{um}p)$$
$$U_{15} = -U_{16} = \overline{F(p)}(V_3 - V_1)Q/(2c_{33}D_{um}p)$$
$$D_{um} = V_1(\alpha_3 W_3 - \alpha_5 W_5) + V_3(\alpha_5 W_5 - \alpha_1 W_1) + V_5(\alpha_1 W_1 - \alpha_3 W_3)$$

$$U^r_{11} = (R_1G_{11} - R_3G_{21} + R_5G_{31})/(D_{sm}e^{j\alpha_1 d})$$
$$U^r_{13} = (R_1G_{13} - R_3G_{23} + R_5G_{33})/(D_{sm}e^{j\alpha_3 d})$$
$$U^r_{15} = (R_1G_{15} - R_3G_{25} + R_5G_{35})/(D_{sm}e^{j\alpha_5 d})$$
$$D_{sm} = D_{11}G_{11} - D_{21}G_{21} + D_{31}G_{31}$$

$$G_{11} = D_{23}D_{35} - D_{33}D_{25}, \quad G_{21} = D_{13}D_{35} - D_{33}D_{15}, \quad G_{31} = D_{13}D_{25} - D_{15}D_{23}$$
$$G_{13} = D_{31}D_{25} - D_{21}D_{35}, \quad G_{23} = D_{31}D_{15} - D_{11}D_{35}, \quad G_{33} = D_{15}D_{21} - D_{11}D_{25}$$
$$G_{15} = D_{21}D_{33} - D_{31}D_{23}, \quad G_{25} = D_{11}D_{33} - D_{31}D_{13}, \quad G_{35} = D_{11}D_{23} - D_{13}D_{21}$$

▲Yong-Yun Kim

Yong Yun Kim received the B.S. degree in mechanical engineering from Yonsei University, Seoul, Korea in 1982 and the M.S. degree in mechanical engineering from University of Toledo, Ohio, U.S.A. in 1989. He received the Ph.D. degree in 1993 and worked as a post doctoral researcher for about one year in aerospace engineering and engineering mechanics from University of Cincinnati, Ohio, U.S.A. Since 1994, he has been with Samsung Aerospace Industries, Kyhung, Korea, where he has been developing several types of interconnecters for semiconductor package. His research-interests are mathematical and experimental modeling of field problems with regard to plastic deformation of thin plate, elastic wave propagation, and vibration and noise.